REPORT DOCUMENTATION PAGE

Form Approved
OMB NO. 0704-0188

1. AGENCY USE ONLY *(Leave blank)*	2. REPORT DATE	3. REPORT TYPE AND DATES COVERED
	9/18/96	Technical

4. TITLE AND SUBTITLE
A Time Integration Algorithm for Flexible Mechanism Dynamics: The DAE α-Method

5. FUNDING NUMBERS
DAAL03-92-G-0247

6. AUTHOR(S)
Jeng Yen, Linda Petzold and Soumyendu Raha

7. PERFORMING ORGANIZATION NAMES(S) AND ADDRESS(ES)
University of Minnesota
Department of Computer Science
4-192 EE/CS Bldg, 200 Union St SE
Minneapolis, MN 55455

8. PERFORMING ORGANIZATION REPORT NUMBER

9. SPONSORING / MONITORING AGENCY NAME(S) AND ADDRESS(ES)
U.S. Army Research Office
P.O. Box 12211
Research Triangle Park, NC 27709-2211

10. SPONSORING / MONITORING AGENCY REPORT NUMBER
ARO 29850.6-MA

11. SUPPLEMENTARY NOTES
The views, opinions and/or findings contained in this report are those of the author(s) and should not be construed as an official Department of the Army position, policy or decision, unless so designated by other documentation.

12a. DISTRIBUTION / AVAILABILITY STATEMENT
Approved for public release; distribution unlimited.

12 b. DISTRIBUTION CODE

13. ABSTRACT *(Maximum 200 words)*
This paper introduces a new family of second-order methods for solving the index-2 DAE equations of motion for flexible mechanism dynamics. These methods, which extend the α-methods for ODEs of structural dynamics to DAEs, possess numerical dissipation that can be controlled by the user. Convergence and stability analysis is given and verifies that the DAE α-methods introduce no additional oscillations and preserve the stability of the underlying ODE system. Convergence of the Newton iteration, which can be a source of difficulty in solving nonlinear oscillartoy systems with large stepsizes, is achieved via a coordinate-split modification to the Newton iterations. Numerical results illustrate the effectiveness of the new methods for simulation of flexible mechanisms.

14. SUBJECT TERMS
constrained dynamics, multibody systems, differential-algebraic equations, numerical methods, highly oscillatory systems

15. NUMBER IF PAGES
22

16. PRICE CODE

17. SECURITY CLASSIFICATION OR REPORT	18. SECURITY CLASSIFICATION OF THIS PAGE	19. SECURITY CLASSIFICATION OF ABSTRACT	20. LIMITATION OF ABSTRACT
UNCLASSIFIED	UNCLASSIFIED	UNCLASSIFIED	UL

DEPARTMENT OF COMPUTER SCIENCE

UNIVERSITY OF MINNESOTA

INSTITUTE OF TECHNOLOGY
UNIVERSITY OF MINNESOTA
4-192 EE/CSci Building
200 Union Street SE
Minneapolis, Minnesota 55455
612/625-4002

TR 96-031

A Time Integration Algorithm for Flexible Mechanism Dynamics: The DAE α-Method

by: Jeng Yen, Linda Petzold, and Soumyendu Raha

Technical Report

Department of Computer Science
University of Minnesota
4-192 EECS Building
200 Union Street SE
Minneapolis, MN 55455-0159 USA

TR 96-031

A Time Integration Algorithm for Flexible Mechanism Dynamics: The DAE α–Method

by: Jeng Yen, Linda Petzold, and Soumyendu Raha

A Time Integration Algorithm for Flexible Mechanism Dynamics: The DAE α-Method *

Jeng Yen Linda Petzold
Soumyendu Raha

Department of Computer Science
and Army High Performance Computing Research Center
University of Minnesota
Minneapolis, MN 55455

April 23, 1996

Abstract

This paper introduces a new family of second-order methods for solving the index-2 DAE equations of motion for flexible mechanism dynamics. These methods, which extend the α-methods for ODEs of structural dynamics to DAEs, possess numerical dissipation that can be controlled by the user. Convergence and stability analysis is given and verifies that the DAE α-methods introduce no additional oscillations and preserve the stability of the underlying ODE system. Convergence of the Newton iteration, which can be a source of difficulty in solving nonlinear oscillatory systems with large stepsizes, is achieved via a coordinate-split modification to the Newton iteration. Numerical results illustrate the effectiveness of the new methods for simulation of flexible mechanisms.

1 Introduction

The numerical solution of flexible multibody systems is required for geometrically nonlinear dynamic analysis of articulated structures. These are structures in which

*The work was partially sponsored by the Army High Performance Computing Research Center under the auspices of the Department of Army, Army Research Laboratory cooperative agreement numbers DAAH04-95-2-0003/contract number DDAH04-95-C-0008, and by ARO contract number DAAH04-94-6-0208 and DAAH04-94-6-0213, the content of which does not necessarily reflect the position or the policy of the government, and no official endorsement should be inferred.

kinematic connections permit large relative motion between components that undergo small elastic deformation. A source of difficulty in the solution of flexible multibody equations of motion is the coupling between the elastodynamic equations and the gross motion. Simulation of flexible multibody systems has been an active research topic for the last two decades. Many of the developments in flexible multibody systems have been implemented in the multibody dynamic analysis codes [19, 21]. For such systems, an important feature of the solution is the nonlinear oscillations induced by the elastodynamics equations. Moreover, since the governing equations of flexible multibody systems are often modeled using algebraic constraints, the numerical solution of differential-algebraic equations (DAE) is required [1, 27]. This paper is concerned with the numerical solution of the DAE of constrained flexible multibody motion by applying the family of α-methods for linear structural dynamics problems.

Recent developments in the simulation of multibody systems have created a variety of methodologies for efficient automation of the process of constructing the highly nonlinear equations of motion of constrained multibody mechanical systems [10],

$$\ddot{q} - f(\dot{q}, q, t) + G^T \lambda = 0 \tag{1.1a}$$

$$g(q, t) = 0 \tag{1.1b}$$

where q is the generalized coordinates, λ is the Lagrange multipliers that couple the kinematic constraints g with the Newton-Euler equations of motion, and $G = \frac{\partial g}{\partial q}$ is the constraint Jacobian. While many contributions to the literature have focused on the efficient generation of (1.1) [10, 14, 20, 21], in recent years there has been progress in the numerical solution of differential-algebraic equations (DAE) [1, 9, 8]. Solution techniques for multibody systems have been proposed in [5, 6, 15, 18, 23, 26]. Two basically different approaches have been proposed in the literature for integration of (1.1). The first involves direct application of *stiffly stable* numerical integration, such as backward differentiation formulas (BDF), to various forms of DAEs derived from (1.1). The second approach is based on the solution of the *state-space* form of (1.1) that is projected onto the constraint manifold.

Time integration algorithms for solving structural dynamics problems have been developed since the late 1950's [17]. General requirements and the foundations of these methods have been well-documented [11, 12, 28, 3]. Although their main application area is to linear structural dynamics, these methods can be directly applied to the initial value problems of *nonlinear* second-order ordinary differential equations (ODE),

$$\ddot{q} = f(\dot{q}, q, t). \tag{1.2}$$

Accuracy and stability analysis hold for the numerical methods, provided the discretized nonlinear equations have been solved accurately, i.e., within a small enough tolerance. For example, the HHT-α method [11] for (1.2) is given by

$$a_{n+1} = (1 + \alpha) f_{n+1} - \alpha f_n \tag{1.3a}$$

$$q_{n+1} = q_n + hv_n + h^2((\frac{1}{2} - \beta)a_n + \beta a_{n+1}) \quad (1.3b)$$

$$v_{n+1} = v_n + h((1-\gamma)a_n + \gamma a_{n+1}) \quad (1.3c)$$

where the subscript denotes the corresponding function value at the time, e.g., $q_n = q(t_n)$, $h = t_{n+1} - t_n$ is the time step, $\alpha \in [-\frac{1}{3}, 0]$, $\beta = \frac{(1-\alpha)^2}{4}$, and $\gamma = \frac{1}{2} - \alpha$. It is well-known that the HHT-α family is second-order accurate and A-stable. Numerical dissipation is maximum for $\alpha = -0.3$, and zero for $\alpha = 0$. Controllable numerical dissipation and unconditional stability are needed to deal with the high-frequency modes which often result from standard finite element spatial discretization. For nonlinear oscillations, these properties are also required in the solution of flexible multibody systems. Rather than using *ad hoc* mode-selection processes, this approach is more desirable because the elimination of higher frequencies is controlled by selection of the parameters.

This paper is concerned with the numerical solution of constrained flexible multibody motion by the family of α-methods. Attempts have been made to apply the HHT-α-method (1.3) directly to (1.1) and its index-2 form [2]. However, these methods are plagued by oscillations which are largely unphysical. Here, we extend the α-method to DAEs in a way which does not introduce additional oscillations. The basic idea of the proposed method is to use the *underlying* ODEs of DAEs and the projection onto the constraint manifold. The main effort is in developing numerical schemes which exploit the structure of multibody dynamic equations, to maintain the stability and reduce the computational cost as compared to a straightforward application. To treat the internal oscillations in the constrained systems, we use a modified Newton-type iteration based on the *Coordinate-Split* formulation of multibody systems [26].

In Section 2, we show the direct application of the α-method to nonlinear multibody DAEs. A projection step to enforce the position and velocity constraints is used for maintaining the stability and accuracy of the numerical solution. A convergence analysis of this approach is given. In Section 3, we describe an effective form of the α-method for constrained flexible multibody equations. In addition, we describe an efficient Newton-type iteration for dealing with the high-frequency oscillations that arise from small elastic deformation. Numerical experiments illustrating the effectiveness of the DAE-α method are given in Section 4.

2 Numerical integration of flexible multibody systems

Based on the spatial discretization of the elastomechanical PDE, the dynamic equations of the response of a discrete model of a structure are given by

$$M^e\ddot{u} + C^e\dot{u} + K^e u = f^e(t) \quad (2.1)$$

where $u \in \mathbb{R}^{n_u}$ is the nodal displacement, $f^e(t)$ is the time-dependent function of applied load, and M^e, C^e and K^e are the mass, damping, and stiffness matrices, respectively. High-frequency vibrations usually result from the spatial discretization. To remove undesired oscillation, the α-method and its variants are designed to achieve controllable numerical dissipation and A-stability. These properties are also important in the numerical solution of flexible multibody systems. In what follows, we formulate an extension of the HHT-α-method to solve the DAEs of constrained multibody systems.

The basic form of constrained multibody equations of motion is given by (1.1), which is a DAE of index-3 (see [1] for the definition of index). Due to the problems of numerical instability in solving index-3 DAEs, most of the solution techniques for (1.1) have been developed using differentiation of the constraints (1.1b). The analytic solution of (1.1) satisfies

$$M(q)\ddot{q} + G^T\lambda - f(\dot{q}, p, t) = 0 \tag{2.2a}$$

$$G(q)\ddot{q} + \frac{\partial G\dot{q}}{\partial q}\dot{q} + 2\frac{\partial^2 g}{\partial q \partial t}\dot{q} + \frac{\partial^2 g}{\partial t^2} = 0 \tag{2.2b}$$

$$G(q)\dot{q} + \frac{\partial g}{\partial t} = 0 \tag{2.2c}$$

$$g(q, t) = 0 \tag{2.2d}$$

where (2.2c) and (2.2b) are the velocity and acceleration constraints, respectively. They are obtained by once and twice differentiating the position constraint (2.2d).

Solving (2.2a) and (2.2b) for $\dot{v}$, the underlying ODE of (2.2) is obtained

$$\ddot{q} = \phi(\dot{q}, q, t) = M^{-1}(f - G^T\lambda) \tag{2.3}$$

where $\lambda = (GM^{-1}G^T)^{-1}(GM^{-1}f - \eta)$ and $\eta = -(\frac{\partial G\dot{q}}{\partial q}\dot{q} + 2\frac{\partial^2 g}{\partial q \partial t} + \frac{\partial^2 g}{\partial t^2})$. For simplicity of notation, we assume that M is invertible. Any conventional numerical integration method can be applied to (2.3), however the numerical solution will not preserve the constraints (2.2c) and (2.2d). To enforce the constraints, the numerical solution can be projected onto the constraint manifold. For an approximation $\tilde{q}$ of $q(t)$, $\tilde{q}$ is projected onto the manifold

$$M(q)(q - \tilde{q}) + G^T(q, t)\tilde{\nu} = 0 \tag{2.4a}$$

$$g(q, t) = 0. \tag{2.4b}$$

This nonlinear system can be solved using Newton-type methods, since its Jacobian is nonsingular near the constraint manifold [10, 15]. For the velocity constraints, the approximation $\tilde{v}$ is projected onto the velocity constraint manifold by solving the linear system

$$M(q)(v - \tilde{v}) + G^T(q, t)\tilde{\mu} = 0 \tag{2.5a}$$

$$G(q, t)v = 0. \tag{2.5b}$$

Remark 2.1 *The projection of $\tilde{q}$ onto the constraint manifold has been proposed by many authors [18, 23]. A variant of (2.4) was used in the half-explicit extrapolation method [15],*

$$M(\tilde{q})(q-\tilde{q}) + G^T(\tilde{q},t)\tilde{\nu} = 0,$$

where $\tilde{q}$ is obtained by extrapolation.

Applying the α-method (1.3) to (2.3), and projecting the numerical solution to (2.4) and (2.5) yields

$$\begin{aligned}
a_{n+1} - (1+\alpha)\phi_{n+1} + \alpha\phi_n &= 0 && \text{(2.6a)}\\
M(\tilde{q}_{n+1})(q_{n+1} - \tilde{q}_{n+1}) + G^T(\tilde{q}_{n+1})\tilde{\nu}_{n+1} &= 0 && \text{(2.6b)}\\
M(\tilde{q}_{n+1})(v_{n+1} - \tilde{v}_{n+1}) + G^T(\tilde{q}_{n+1})\tilde{\mu}_{n+1} &= 0 && \text{(2.6c)}\\
G(q_{n+1})v_{n+1} &= 0 && \text{(2.6d)}\\
g(q_{n+1}) &= 0 && \text{(2.6e)}
\end{aligned}$$

where

$$\begin{aligned}
\tilde{q}_{n+1} &= q_n + hv_n + h^2((\frac{1}{2}-\beta)a_n + \beta a_{n+1}) && \text{(2.7a)}\\
\tilde{v}_{n+1} &= v_n + h((1-\gamma)a_n + \gamma a_{n+1}). && \text{(2.7b)}
\end{aligned}$$

For simplicity, we assume that the kinematic constraints do not depend explicitly on time, e.g., scleronomic constraints. The accuracy and stability of (2.6) can be shown by the standard analysis of (1.3) and Gauss-Newton iteration of the constraints.

Theorem 2.1 *Suppose g is smooth, e.g., $g \in C^2$, $G = \frac{\partial g}{\partial q}$ has full row rank on the constraint manifold, and GMG^T is invertible. Let c_ϕ be the Lipschitz constant of the function ϕ of (2.3), i.e.,*

$$\|\phi(a) - \phi(b)\| \le c_\phi \|a - b\|.$$

There exists h_0 such that for $h \le h_0$ the solutions q_{n+1} and v_{n+1} of (2.6) satisfy

$$\|q_{n+1} - q(t_{n+1})\| = O(h^2), \quad \|v_{n+1} - v(t_{n+1})\| = O(h) \qquad (2.8)$$

given consistent starting values $(q_0, v_0, a_0, \tilde{\nu}_0, \tilde{\mu}_0)$.

Proof. Applying the numerical integration of (1.3) to the underlying ODE of (2.2), we denote $\tilde{X}_{n+1} = [\tilde{q}_{n+1}, h\tilde{v}_{n+1}, h^2\tilde{a}_{n+1}]$, where

$$\tilde{a}_{n+1} = (1+\alpha)\phi(\tilde{q}_{n+1}, \tilde{v}_{n+1}, t_{n+1}) - \alpha\phi(\tilde{q}_n, \tilde{v}_n, t_n),$$

and $\tilde{q}_{n+1}$ and $\tilde{v}_{n+1}$ are obtained from (2.7) using $\tilde{a}_{n+1}$. Linearization of the HHT α-method yields

$$\tilde{X}_{n+1} = A_n \tilde{X}_n \ , \quad n \in \{0, 1, 2, ..., N\}. \qquad (2.9)$$

where A_i for $i \in \{0,1,2,....,N\}$ is the *local amplification matrix*. For a linear function $\phi = M^{-1}Kq$, standard analysis [11] shows that the local truncation error of $\tilde{X}_{n+1}$ is $O(h^3)$, with α, β, γ given in (1.3). Since ϕ is Lipschitz, eigenvalue analysis for the linear model function can be applied to the nonlinear case by the linearization of (2.9), see [2] for details.

Since GMG^T is nonsingular and G has full row rank, locally there exists $P(q)$ such that $P(q)G^T(q) = 0$. Premultiplying (2.6b,2.6c) by $\tilde{P}_{n+1} = P(\tilde{q}_{n+1})$ yields

$$\begin{pmatrix} \tilde{P}_{n+1}M(\tilde{q}_{n+1})(q_{n+1} - \tilde{q}_{n+1}) \\ \tilde{P}_{n+1}M(\tilde{q}_{n+1})(v_{n+1} - \tilde{v}_{n+1}) \end{pmatrix} = 0,$$

which is a *state-space* ODE of (1.1). The state-space solution together with the constraints (2.6d,2.6e) is well-defined. In addition, the local error of (q_{n+1}, hv_{n+1}) is the same order as that of $(\tilde{q}_{n+1}, h\tilde{v}_{n+1})$, provided that the nonlinear system is solved with an error tolerance which is less than the truncation error. For more details on the proof, we refer to [24] (Theorem 3, pp. 559-561). Since $\tilde{X}_{n+1}$ is obtained from the second-order α-method, this implies that the local error of $[q_{n+1}, hv_{n+1}]$ is $O(h^2)$, provided that the nonlinear equations are solved with an error tolerance $O(h^3)$. Denoting $X_{n+1} = [q_{n+1}, hv_{n+1}, h^2a_{n+1}]$, we conclude that the local truncation error of X_{n+1} is $O(h^3)$. It follows that (2.8) holds for $h \leq h_0$, where h_0 depends on c_ϕ and on the Jacobian and Hessian of g. □

Remark 2.2 *The above results hold for many of the numerical integration methods of structural dynamics, including the Newmark β-method [17], and a variety of the α-methods [12, 28, 3].*

Note that the projection $\tilde{P}_{n+1}$ can be replaced by $P_{n+1} = P(q_{n+1})$ in the above analysis [18]. Therefore, we may use $M(q_{n+1})$ and $G^T(q_{n+1})$ in (2.6b,2.6c) instead of $M(\tilde{q}_{n+1})$ and $G^T(\tilde{q}_{n+1})$.

Remark 2.3 *For the one-step α-methods, the error of the multipliers $(\tilde{\nu}_{n+1}, \tilde{\mu}_{n+1})$ does not depend on accumulated errors of the constraints from the past state variables. Consider the expansion of the constraints $g(\tilde{q}_{n+1})$ about q_n*

$$g(\tilde{q}_{n+1}) = g(q_{n+1}) + G(q_{n+1})(q_{n+1} - \tilde{q}_{n+1} + \xi_{n+1})$$

for some $\|G_{n+1}\xi_{n+1}\| = O(\|q_{n+1} - \tilde{q}_{n+1}\|^2)$. Using the projection (2.4), the associated multipler $\tilde{\nu}_{n+1}$ is given by

$$\tilde{\nu}_{n+1} = (G_{n+1}M_{n+1}^{-1}G_{n+1}^T)^{-1}(g(\tilde{q}_{n+1}) - G_{n+1}\xi_{n+1}). \tag{2.10}$$

Similarly, the projection (2.5) yields the multiplier

$$\tilde{\mu}_{n+1} = (G_{n+1}M_{n+1}^{-1}G_{n+1}^T)^{-1}(G_{n+1}\tilde{v}_{n+1}). \tag{2.11}$$

Equations (2.6) illustrate a straightforward application of the α-method to the constrained multibody systems. However, the computational cost of this approach is relatively large for moderate- to large-scale multibody systems. Each iteration of (2.6) requires the inversion of the mass-inertia matrix M and the formation of f and decomposition of $GM^{-1}G^T$ in the computation of ϕ_{n+1}, e.g., the underlying ODE (2.3). To remedy the high cost of (2.6), we retain the *Lagrange multipiler* λ in (1.1) to avoid the inversion of large matrices. This is achieved because the linear algebra involved in the computation of ϕ_{n+1} is the same as those in the projection steps of (2.4) and (2.5). It will be shown in the next section how this approach leads to the *DAE* α-method which applies the discretization schemes of the α-methods in linear structural dynamics to the index-2 DAE of the constrained multibody equations of motion.

3 The DAE α-method

One can reduce the computational cost of (2.6) by eliminating the explicit solution for ϕ_{n+1}. Substituting the right-hand side of (2.3) into (2.6a) yields

$$a_{n+1} = (1+\alpha)M_{n+1}^{-1}(f_{n+1} - G_{n+1}^T\lambda_{n+1}) - \alpha\phi_n \tag{3.1}$$

where $\phi_n = M_n^{-1}(f_n - G_n^T\lambda_n)$. Substituting (3.1) into (2.7) yields

$$\tilde{q}_{n+1} = q_n + hv_n + h^2[(\frac{1}{2}-\beta)a_n - \beta\alpha\phi_n] + h^2\hat{\beta}M_{n+1}^{-1}(f_{n+1} - G_{n+1}^T\lambda_{n+1}) \tag{3.2a}$$

$$\tilde{v}_{n+1} = v_n + h[(1-\gamma)a_n - \gamma\alpha\phi_n] + h\hat{\gamma}M_{n+1}^{-1}(f_{n+1} - G_{n+1}^T\lambda_{n+1}) \tag{3.2b}$$

where $\hat{\beta} = \beta(1+\alpha)$ and $\hat{\gamma} = \gamma(1+\alpha)$. Substitute (3.2) into (2.6b, 2.6c) to obtain the DAE *α-method*

$$M_{n+1}(q_{n+1} - \hat{q}_n) - \hat{\beta}h^2 f_{n+1} + G_{n+1}^T\nu_{n+1} = 0 \tag{3.3a}$$

$$M_{n+1}(v_{n+1} - \hat{v}_n) - \hat{\gamma}h f_{n+1} + G_{n+1}^T\mu_{n+1} = 0 \tag{3.3b}$$

$$G_{n+1}v_{n+1} = 0 \tag{3.3c}$$

$$g(q_{n+1}) = 0 \tag{3.3d}$$

where

$$\hat{q}_n = q_n + hv_n + h^2[(\frac{1}{2}-\beta)a_n - \beta\alpha\phi_n] \tag{3.4a}$$

$$\hat{v}_n = v_n + h[(1-\gamma)a_n - \gamma\alpha\phi_n], \tag{3.4b}$$

and $a_0 = \phi_0$ and $a_n = (1+\alpha)\phi_n + \alpha\phi_{n-1}$ for $n \geq 1$. Note that ν_{n+1} and μ_{n+1} in (3.3) comprise $h^2\hat{\beta}\lambda_{n+1}$ and the corresponding *correction* terms by the projections.

Comparing (3.3) to (2.6), the solutions of the state variables q_{n+1} and v_{n+1} differ by the use of two slightly different projections. The solution of (3.3) is obtained from

the projection along the direction of $M_{n+1}^{-1}G_{n+1}^T$, while the solution of (2.6) is obtained form the projection along the direction of $\tilde{M}_{n+1}^{-1}\tilde{G}_{n+1}^T$. On a smooth manifold, e.g. $g \in C^2$, the distance between the solutions can be bounded by $O(h)$ for $h \leq h_0$, [18, 24]. However, the *algebraic* variables ν_{n+1} and μ_{n+1} contain also the scaled Lagrange multipier λ of (1.1) which was not accounted for by $\tilde{\nu}_{n+1}$ and $\tilde{\mu}_{n+1}$ in (2.6b) and (2.6c), respectively. Thus, convergence analysis of the *algebraic* variables (ν_{n+1}, μ_{n+1}) remains for the accuracy and stability of the DAE α-method (3.3). It can be shown via the results for the application of the *stiffly stable* numerical integration methods to index-2 DAEs [9].

Theorem 3.1 *Let the assumptions of Theorem 2.1 hold, and the initial value* (q_0, v_0) *at* t_0 *satisfy*

$$\|q_0 - q(t_0)\| = O(h^3) \ , \quad \|v_0 - v(t_0)\| = O(h^2)$$

and $g(q_0) = 0$, $G(q_0)v_0 = 0$. *The corresponding initial values of the multipliers are*

$$\nu_0 = \hat{\beta}h^2\lambda_0 \ , \quad \mu_0 = \hat{\gamma}h\lambda_0,$$

where $\lambda_0 = \lambda(t_0)$ *of (1.1). There exists* h_0 *such that for* $h \leq h_0$ *the solution of (3.3) satisfies*

$$\|q_n - q(t_n)\| = O(h^2) \ , \quad \|v_n - v(t_n)\| = O(h)$$

for all $n \in \{0, 1, 2, ..., N\}$.

Proof. The algebraic variables of (3.3) can be written as

$$\nu_{n+1} = \tilde{\nu}_{n+1} + \hat{\beta}h^2\lambda_{n+1},$$

$$\mu_{n+1} = \tilde{\mu}_{n+1} + \hat{\gamma}h\lambda_{n+1}$$

where $\tilde{\nu}_{n+1}$ and $\tilde{\mu}_{n+1}$ are due to the projections of $\tilde{q}_{n+1}$ and $\tilde{v}_{n+1}$ onto the corresponding constraint manifolds, i.e., (2.4) and (2.5), respectively. Using the compact form of (2.9), e.g., $X_{n+1} = A_n X_n$, the discretization of (3.3) can be expressed by

$$q_{n+1} = q_n + hv_n + \frac{h^2}{2}a_n + \delta_{n+1} + G_{n+1}^T\tilde{\nu}_{n+1} \tag{3.5a}$$

$$v_{n+1} = v_n + ha_n + \frac{\gamma}{\beta h}\delta_{n+1} + G_{n+1}^T\tilde{\mu}_{n+1} \tag{3.5b}$$

$$a_{n+1} = a_n + \frac{1}{\beta h^2}\delta_{n+1} \tag{3.5c}$$

where

$$\delta_{n+1} = \beta h^2[(1+\alpha)(M_{n+1}^{-1}(f_{n+1} - G_{n+1}^T\lambda_{n+1}) - \alpha\phi_n - a_n].$$

Applying the test equation $\ddot{q} = -\omega^2 q$ to (3.5), three eigenvalues of the amplification matrix A_n as $h\omega^2 \to \infty$ are of the magnitudes [2]

$$\{\frac{\alpha}{1+\alpha}, \frac{1-\alpha}{1+\alpha}, \frac{1-\alpha}{1+\alpha}\}$$

for $\beta = \frac{(1-\alpha)^2}{4}$ and $\gamma = \frac{1}{2} - \alpha$. Thus, the α-method is stiffly stable for all $\alpha \in [-\frac{1}{3}, 0)$. Convergence of stiffly stable integration methods for index-2 DAEs is well-known [9]. These results yield the convergence of the algebraic variables in (3.5). In addition, for the special case $\alpha = 0$, i.e., the *implicit trapezoidal rule*, the eigenvalues corresponding to $(\tilde{q}_{n+1}, h\tilde{v}_{n+1})$ are 1 and 0. Convergence analysis has also been carried out for this case (for example see [13]).

Using these results and Theorem 2.1, the local errors of ν_{n+1} and μ_{n+1} can be obtained from (2.10) and (2.11), respectively. Consequently, (3.1) implies that

$$\|\lambda_{n+1} - \lambda(t_{n+1})\| = O(h)$$

where $\lambda(t_{n+1})$ is defined by (2.3). For $\|X_n - X(t_n)\| = O(h^3)$, we conclude that

$$\|\tilde{q}_{n+1} - q(t_{n+1})\| = O(h^3) \ , \quad \|\tilde{v}_{n+1} - v(t_{n+1})\| = O(h^2)$$

where $\tilde{q}_{n+1}$ and $\tilde{v}_{n+1}$ are the solutions of (3.2). Thus, the solution of (3.3) satisfies $\|q_{n+1} - q(t_{n+1})\| = O(h^2)$ and $\|v_{n+1} - v(t_{n+1})\| = O(h)$, $\forall n \in 0, 1, ..., N-1$. □

3.1 Coordinate-split formulation

Alternatively, we can directly apply the α-method to an index-1 form of (1.1) using nonlinear projection operators, e.g., an annihilation matrix $P(q)$ such that $P(q)G^T(q) = 0$. Premultiplying (3.3a) and (3.3b) by such a matrix yields

$$\begin{aligned} P(q_{n+1})(M_{n+1}(q_{n+1} - \hat{q}_n) - \hat{\beta}h^2 f_{n+1}) &= 0 && \text{(3.6a)} \\ P(q_{n+1})(M_{n+1}(v_{n+1} - \hat{v}_n) - \hat{\gamma}h f_{n+1}) &= 0 && \text{(3.6b)} \\ G_{n+1}v_{n+1} &= 0 && \text{(3.6c)} \\ g(q_{n+1}) &= 0. && \text{(3.6d)} \end{aligned}$$

Accuracy and stability of the α-methods for ODE are preserved, since the algebraic variables have been annihilated.

There is a potential gain in efficiency for this formulation due to the size-reduction of the nonlinear system, compared to (3.3). *An important practical consequence of (3.6) is that (ν, μ) have been eliminated from the DAE.* Thus, the Newton iteration convergence test in a numerical implementation of (3.6) no longer needs to include those multipliers, which can cause problems in the direct numerical solution of (3.3). One could in principle also consider removing (ν, μ) from the Newton convergence test in the solution of (3.3), however it is not usually possible to justify this action. Elimination of these variables from the Newton convergence test in the solution of (3.3) can lead to a code which sometimes produces incorrect solutions. It is the fact that multiplying by the *nonlinear* $P(q)$ eliminates (ν, μ) from the nonlinear system, which allows these variables to be excluded from the tests in the solution of (3.6).

However, the computation of the matrix $P(q)$ and its derivative can be costly if not impossible. We have dealt with this problem by an efficient Newton-type iteration of (3.6) using a family of the CS-matrix $P(q)$ [26].

To obtain a cheap representation of $P(q)$ and its derivative, the CS-operator is computed by the solution of a class of pseudo-inverses of the constraint Jacobian $G(q)$.

Definition 3.1 *[Coordinate-Splitting Matrix] Let X and Y be the matrices whose columns constitute the standard basis such that $\|(G(q)Y)^{-1}\|$ is bounded in a neighborhood U_0 of q_0. The* coordinate-splitting matrix *is defined by*

$$P(q) = X^T - Q(q)^T Y^T = X^T(I - G(q)^T(G(q)Y)^{-T}Y^T) \tag{3.7}$$

where $Q(q) = (G(q)Y)^{-1}G(q)X$.

Remark 3.1 *From the construction of the CS matrix $P(q)$, one can easily see that $P(q)G^T(q) = 0$ for all q, i.e., $P(q)$ is orthogonal to range(G^T). Furthermore, the row vectors of $P(q)$ are orthonormal, i.e., $P(q)^T P(q)$ is the identity.*

The computation of $P(q)$ can be carried out using the LU-factorization of the constraint Jacobian matrix. Applying Gaussian elimination with row-pivoting to G^T yields

$$E_m \cdots E_1 G^T = L_m \cdots L_1 U \tag{3.8}$$

where E_i is the elementary permutation and L_i is a Gauss transformation, $i \in \{1, 2, ..., m\}$. From the factorization, we have

$$[Y, X] = E = E_m \cdots E_1. \tag{3.9}$$

Using the standard solution technique by LU-decomposition, the projected vector $P(q)r$ can computed in a straightforward and relatively cheap way. In addition, the derivative $\frac{dP(q)r}{dq}$ can be computed by the same factorization of G^T and the intermediate result $s = -(GY)^{-1}Y^T r$ from the computation of $P(q)r$.

Remark 3.2 *Alternatively, one can apply QR-factorization to G^T for the computation of $P(q)r$. Using QR-factorization with partial column pivoting [7], we obtain*

$$G^T \tilde{E}_1 \cdots \tilde{E}_m = \tilde{L}_1 \cdots \tilde{L}_m \tilde{U} \tag{3.10}$$

where $\tilde{E}_i$ is the elementary permutation, $\tilde{L}_i$ is the Householder matrix, $i \in \{1, 2, ..., m\}$, and $\tilde{U}$ is upper triangular. The last $(n - m)$ columns of the orthogonal matrix $\tilde{L} = \prod_{i=1}^{m} \tilde{L}_i$ constitute a basis for the null-space of G. Thus we can write

$$\left[\tilde{Y}, \tilde{X}\right] = \tilde{L} = \tilde{L}_1 \cdots \tilde{L}_m. \tag{3.11}$$

Note that $\tilde{X}$ and $\tilde{Y}$ are usually subsets of the standard basis in $\mathbb{R}^n$.

An efficient implementation of Newton-type iteration for (3.6) has been presented in [26], where the Jacobian of the nonlinear system was derived. More importantly, a modification of the Jacobian was obtained to enhance the convergence of Newton-type iterations for high-frequency oscillations. This is achieved by eliminating the term

$$\frac{dP(q)r}{dq} = P(q)\frac{dG^T(q)s}{dq} \equiv 0,$$

where $s = -(GY)^{-1}Y^T r$, from the Jacobian. This term represents the sensitivity of the *potential force* due to the constraints. When the solution is not close to an *equilibrium* on the constraint manifold, this term can be dominant in the Jacobian of the nonlinear system. Consequently, the iterative solution is forced to resolve the high-frequency oscillations if the constraint violation is large compared to the amplitude of the high modes. In highly oscillatory flexible multibody systems, this problem can occur at larger time integration stepsizes. Using the modification of the CS iteration, abbreviated CM, the DAE α-method in the form of (3.6) permits a fast convergence of the solution. In addition, the computational cost of the CS-matrix is insignificant compared to one iteration of (3.3) for DAEs with a small number of constraints, such as large-scale flexible multibody systems. We will present several numerical examples involving high-frequency vibrations to illustrate the advantages of the CM iteration in the next section.

4 Numerical examples

The DAE HHT α-method in (3.3) can be used for any numerical integration scheme for linear structural dynamics. For the numerical solution of the test problems, we will use the DAE formulas which are extensions of the *generalized α-method* [3]. The generalized α-method for (1.2) is given by

$$(1-\alpha_m)a_{n+1} + \alpha_m a_n = (1-\alpha_f)f_{n+1} + \alpha_f f_n, \tag{4.1}$$

where the position and velocity states are defined by (1.3b) and (1.3c), respectively. The parameters of the method are obtained by a user-specified value of high-frequency dissipation $\rho \in [0,1]$ (i.e., $\rho = 0$ maximum dissipation, $\rho = 1$ none), such that

$$\alpha_m = \frac{2\rho - 1}{\rho + 1}, \quad \alpha_f = \frac{\rho}{\rho + 1},$$

$$\gamma = \frac{1}{2} - \alpha_m + \alpha_f, \quad \beta = \frac{(1 - \alpha_m + \alpha_f)^2}{4}.$$

This yields a second-order, A-stable family of numerical integration methods. Using (4.1) in (3.3) or (3.6), we need only replace (3.4) by

$$\hat{q}_n = q_n + hv_n + h^2[(\frac{1}{2} - \frac{\beta}{1-\alpha_m})a_n - \frac{\beta\alpha_f}{1-\alpha_m}\phi_n] \tag{4.2a}$$

$$\hat{v}_n = v_n + h[(1 - \frac{\gamma}{1-\alpha_m})a_n - \frac{\gamma\alpha_f}{1-\alpha_m}\phi_n], \tag{4.2b}$$

and $\hat{\beta} = \beta\frac{1-\alpha_f}{1-\alpha_m}$, $\hat{\gamma} = \gamma\frac{1-\alpha_f}{1-\alpha_m}$. The generalized α-method is parametrized by the size of the dominant eigenvalue(s) ρ of its amplification matrix $A(-(h\omega)^2)$ as $h\omega \to 0$. It gives the most comprehensive range of the user-specified value of the spectral radius in the high-frequency limit, while low-frequency dissipation is minimized [3].

4.1 Stiff spring pendulum

To demonstrate the user-specified high-frequency dissipation in the generalized α-method, we use the *stiff pendulum* example. In Cartesian coordinates, a simple stiff pendulum model, with unit mass and gravity, may be expressed as

$$0 = \dot{x} - u \tag{4.3a}$$
$$0 = \dot{y} - v \tag{4.3b}$$
$$0 = \dot{u} + x\lambda \tag{4.3c}$$
$$0 = \dot{v} + y\lambda - 1.0 \tag{4.3d}$$
$$\epsilon^2\lambda = \frac{\sqrt{x^2+y^2} - 1.0}{\sqrt{x^2+y^2}} \tag{4.3e}$$

where the stiff spring of natural length 1.0 and stiffness $\frac{1}{\epsilon^2}$ is attached to the center of mass of the pendulum. Denote by h the stepsize, δ the maximum deflection of the spring, and the potential energy of the system

$$V = \frac{1}{2\epsilon^2}(\sqrt{x^2+y^2} - 1)^2.$$

Then the frequency ω of the system is proportional to $\|dV\|$ such that

$$\frac{1}{\epsilon}\sqrt{\frac{\delta}{1+\delta}} \le \omega \le \frac{1}{\epsilon}\sqrt{\frac{\delta}{1-\delta}}.$$

As $\epsilon \to 0$, the dominant pair of eigenvalues approaches $\pm\infty$ along the imaginary axis. This problem is discussed in more detail in [25].

The numerical solution of the index-1 DAE (4.3) has been carried out applying the generalized α-method to (3.3). Using the initial values $(x_0, y_0, u_0, v_0) = (0.9, 0, 0, 0)$, $\epsilon^2 = 10^{-3}$, and Newton iteration with tolerance 10^{-10}, the results of several combinations of the high frequency dissipation ρ and steplength h for a 0 to 5 second simulation are given. The total energy is plotted in Figure 4.1, with the high-frequency dissipation parameter ρ varying from 1 to 0. The solution trajectory on the coordinate plane is shown in Figure 4.2 with the stepsize varying from 10^{-3} to 10^{-1}. The results illustrate the effective damping of the DAE-α method. As $\rho \to 0$ or the stepsize h is increased, the numerical solution approaches the equilibrium of the spring

while maintaining the slow swing, e.g., see Figure 4.2. Since the accuracy of the numerical solution is second-order, the increasing error in the total energy corresponds to increasing h in the picture. The controllable damping of the DAE α-method is demonstrated by the stiff spring pendulum example. However, the stepsize may be restricted to the convergence of the nonlinear equations resulting in the discretization. In the next subsection, we present a nonlinear bushing example, which illustrates that the CM iteration of (3.6) achieves better convergence than solution of (3.3) via Newton iteration, thus allowing effective damping of high-frequency oscillations by taking larger time steps.

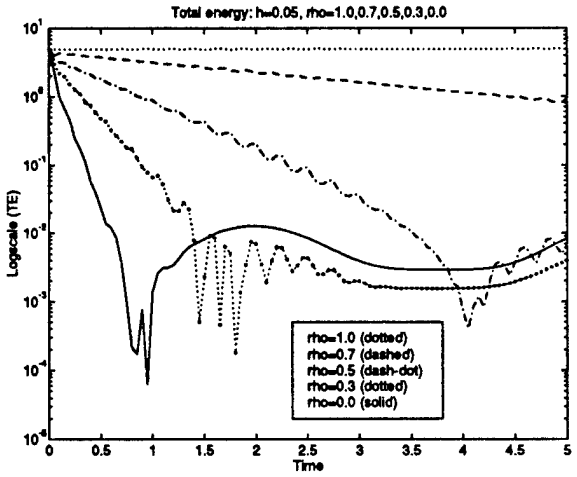

Figure 4.1: Stiff Spring Pendulum Example; $\epsilon^2 = 10^{-3}$, $TOL = 10^{-10}$

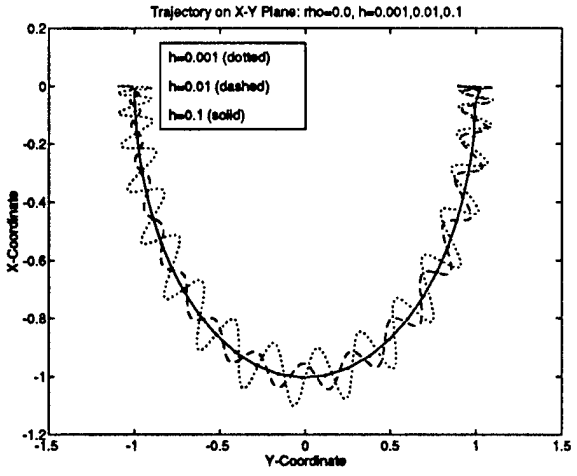

Figure 4.2: Stiff Spring Pendulum Example; $\epsilon^2 = 10^{-3}$, $TOL = 10^{-10}$

4.2 Nonlinear bushing force

The next example is a nonlinear three-variable bushing example. Using 2-D Cartesian coordinates, the problem may be represented as

$$0 = \ddot{x} - \frac{1}{\epsilon^2} f_x \tag{4.4a}$$

$$0 = \ddot{y} - \frac{1}{\epsilon^2} f_y - 1 \tag{4.4b}$$

$$0 = \ddot{\theta} + \frac{1}{10\epsilon^2}\theta - \frac{1}{2}(\cos\theta(\frac{1}{\epsilon^2} f_y + 1) - \sin\theta \frac{1}{\epsilon^2} f_x) \tag{4.4c}$$

$$0 = x^2 + y^2 - 1 \tag{4.4d}$$

where $f_x = \frac{1}{2} - x + \frac{1}{2}\cos\theta$, $f_y = -y + \frac{1}{2}\sin\theta$, and $\epsilon = 10^{-5}$. This problem was solved using both the stabilized index-2 DAE (3.3) and the CM iteration of (3.6). Both the formulations work well for the problem. The CM iteration permits a larger stepsize and therefore a much quicker dissipation. Some results are compared in Figures 4.3 and 4.4. With the initial values $x = 0.8$, $y = 0.6$ and $\theta = 0.0$ and the tolerance for the Newton convergence 10^{-7}, the figures show the response of the θ variable for different parametric values. The simulation was run for $T = 40\pi \times 10^{-5}$ seconds, i.e., roughly 6 cycles of θ and around 20 cycles for x and y.

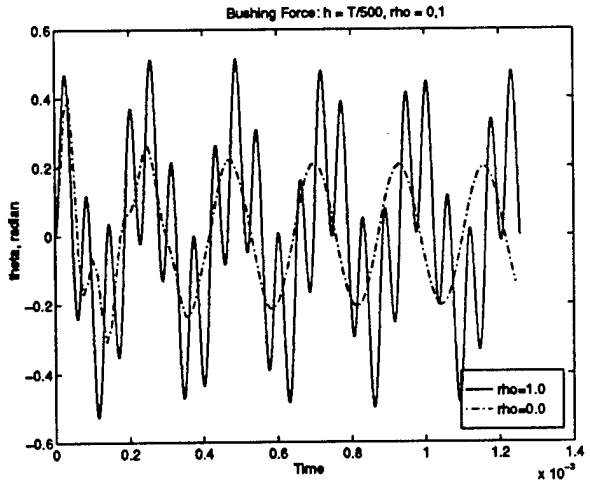

Figure 4.3: Bushing Example, Stabilized Index-2 Formulation; $\epsilon = 10^{-5}$, $TOL = 10^{-7}$

The CS iteration is implemented using $P = \begin{pmatrix} 1 & -y/x & 0 \\ 0 & 0 & 1 \end{pmatrix}^T$, since $x \approx 1$ during the simulation. In Table 4.1, we list the damping measurement of the solution of the CM iteration and that of (3.3). It is measured by the ratio of the initial energy and the energy retained at the end of the simulation. Because a straightforward measurement

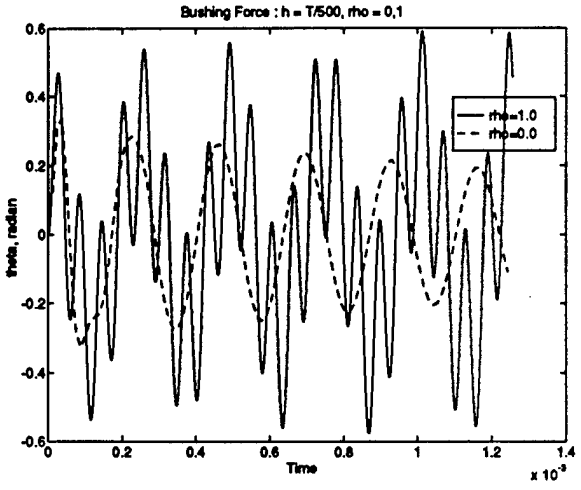

Figure 4.4: Bushing Example, CM Iteration for 500 Timesteps; $\epsilon = 10^{-5}, TOL = 10^{-7}$

No. steps	$\rho = 0$ (CM)	$\rho = 0$	$\rho = \frac{1}{2}$ (CM)	$\rho = \frac{1}{2}$	$\rho = \frac{3}{4}$ (CM)	$\rho = \frac{3}{4}$
200	0.10	0.15	0.35	0.56	0.76	0.90
500	0.24	0.30	0.40	0.65	0.81	0.93
1200	0.30	0.41	0.51	0.76	0.89	0.96
max. h_0	$\frac{T}{40}$	$\frac{T}{100}$	$\frac{T}{70}$	$\frac{T}{150}$	$\frac{T}{80}$	$\frac{T}{175}$

Table 4.1: Final Energy vs. Initial Energy for the Bushing Problem; $T = 40\pi \times 10^{-5}$

of damping from the displacement response is difficult, the energy norm has been conveniently used. The last row of Table 4.1 shows the maximum stepsize that can be taken without causing a failure in Newton convergence. For this example, the CM iteration allows stepsizes twice as large as those of the index-2 formulation. In addition, the CM solution exhibits more rapid convergence towards the *slow solution*, e.g., approaching a smaller energy level than that of (3.3). This is illustrated in Table 4.1, where the same h and ρ were used for both CM and (3.3) solutions.

4.3 Flexible slider-crank

A flexible slider-crank mechanism is presented schematically in Figure 4.5. The mechanism consists of a rigid crank connected with a flexible rod driving a slider on a straight line. Three coordinates (ϕ_1, ϕ_2, x_3) are used for the rigid body equations of motion, and the flexible rod is modeled by a finite element approximation of a linearized Bernoulli-Euler beam. For the details of this model, we refer to [22].

Using a simple beam obtained from the linearization with respect to the vertical displacement by setting the longitudinal displacement to zero, the two constraint

equations are

$$g(q) = \begin{pmatrix} l_1 \sin\phi_1 + l_2 \sin\phi_2 + q_{2k+1} \cos\phi_2 \\ x_3 - l_1 \cos\phi_1 - l_2 \cos\phi_2 + q_{2k+1} \sin\phi_2 \end{pmatrix}$$

where l_1 is the length of the crank, l_2 is the length of the rod, q_j are the nodal coordinates induced by the k elements and q_{2k+1} is the nodal coordinate at the *boundary*. Since the constraint involves only the boundary nodes, the computation of $P(q)$ for the CS formulation can be reduced to

$$\bar{P}(q) = \bar{X}^T - \begin{pmatrix} 0 & \cos\phi_2 \\ 1 & \sin\phi_2 \end{pmatrix} \begin{pmatrix} l_1 \cos\phi_1 & l_2 \cos\phi_2 - q_{2k+1} \sin\phi_2 \\ l_1 \sin\phi_1 & l_2 \sin\phi_2 + q_{2k+1} \cos\phi_2 \end{pmatrix}^{-1} \bar{Y}^T \qquad (4.5)$$

where $\bar{X}^T$ consists of the column vectors e_3 and e_{2k+1} and $\bar{Y}^T$ consists of e_1 and e_2 such that e_j is the jth standard base of $\mathbb{R}^{2k+5}$. The matrix $\bar{P}(q)$ is applied directly to the 4×1 vectors of $X_s^T(M(q) - f)$ with $X_s^T = (e_1, e_2, e_3, e_{2k+1})$. The rest of the $2k + 1$ equations remain unchanged. The computational cost of the CS-matrix P is equivalent to that of $\bar{P}$. Increasing the number of elements, the computation of $\bar{P}$ remains unchanged.

A one-second simulation was run with a driving torque of 0.2 N-m from 0-0.3 second. The initial velocity and all position values are zero except $x_3 = 0.45$. The Newton iteration tolerance was set to 10^{-9}. The spatial discretization of the flexible rod was carried out using $k = 4$, where the magnitude of the maximum eigenvalue is about 1.3×10^4. Using (4.5) in the CM iteration, Newton convergence can be attained with larger stepsizes compared to the index-2 DAE form, see Table 4.2. The high-frequency oscillation of the nodal coordinates is shown in Figure 4.6, where the amplitude of the vibrations is small compared to the rigid motion. The numerical solution corresponding to the slow motion, i.e., (ϕ_1, ϕ_2, x_3), is preserved by the iterations of CM and stabilized index-2 DAE, as shown by the ϕ_2 plots in Figure 4.7. The stepsize $h = \frac{1}{2000}$ is about one period of the highest frequency. Applying stronger damping to the high frequency modes, the solution at the midpoint of the flexible rod is presented in Figure 4.8 with $\rho = 0.5, 0.0$ and $h = \frac{1}{500}$. The high modes are eliminated in the numerical solution, comparing to Figure 4.6. For various combinations of ρ and h, the total energy plots are presented in Figures 4.9 and 4.10. At various levels of damping corresponding to the different values of ρ and h, only the higher modes are removed in the numerical solution. It is shown in Figure 4.11 that faster numerical dissipation of the high modes is achieved via the CM iteration, where $h = \frac{1}{500}$ and $\rho = 0.75$.

Newton Solution Tolerance	h_0 (CM)	h_0 (Index-2 DAE)
10^-5	$\frac{1}{100}$	$\frac{1}{175}$
10^-7	$\frac{1}{250}$	$\frac{1}{500}$
10^-9	$\frac{1}{400}$	$\frac{1}{800}$

Table 4.2: Maximum Stepsize: CM vs. Index-2 DAE, $\rho = 0.75$

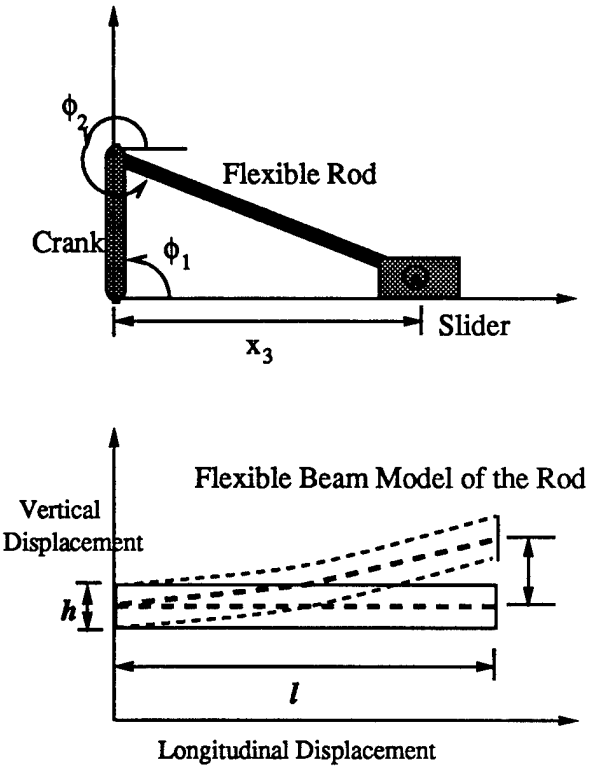

Figure 4.5: Slider-Crank Mechanism with a Flexible Rod

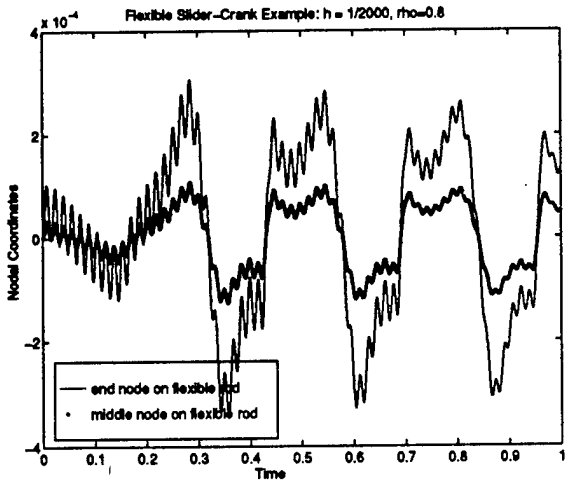

Figure 4.6: Nonlinear Oscillations in Nodal Coordinates

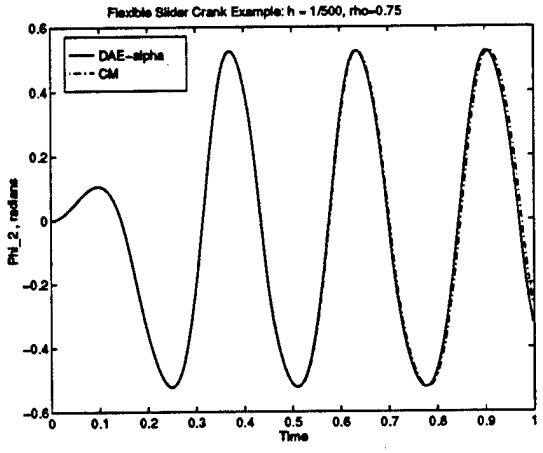

Figure 4.7: Rigid Motion of Coordinate ϕ_2

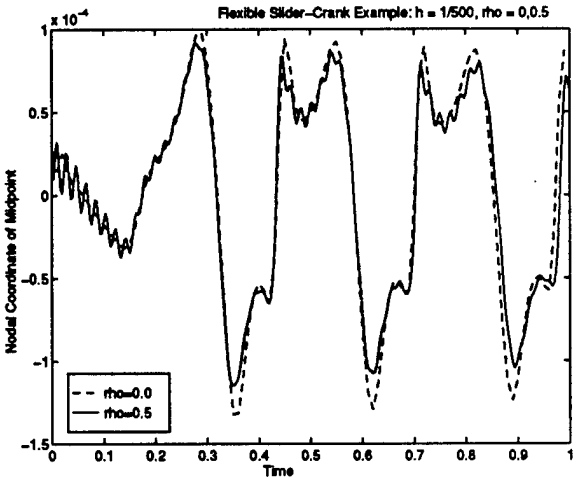

Figure 4.8: Damped Vibration on Midpoint of Flexible Rod

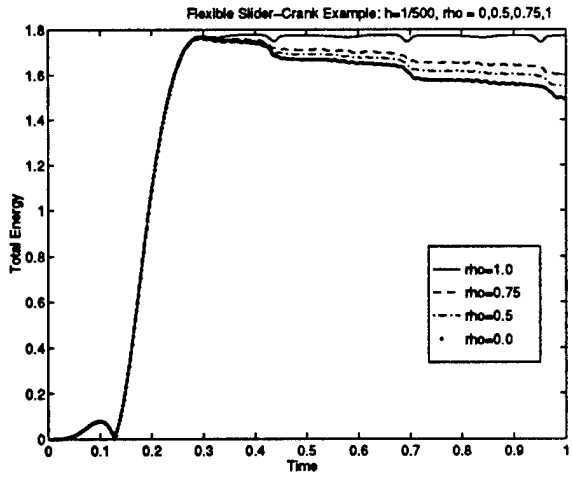

Figure 4.9: Total Energy Comparison, $\rho = 0,0.5,0.75,1.0$

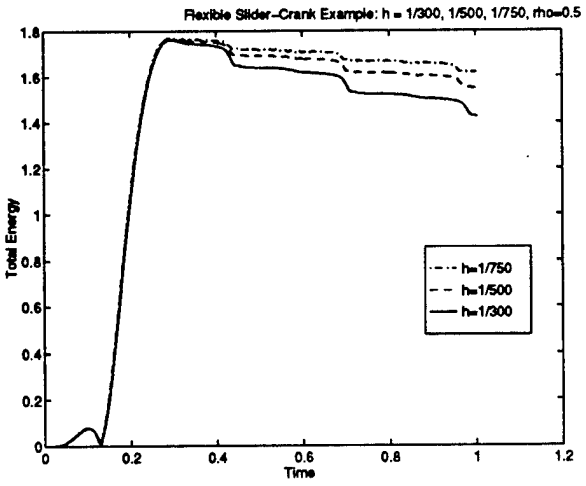

Figure 4.10: Total Energy Comparison, $h = \frac{1}{300}, \frac{1}{500}, \frac{1}{750}$

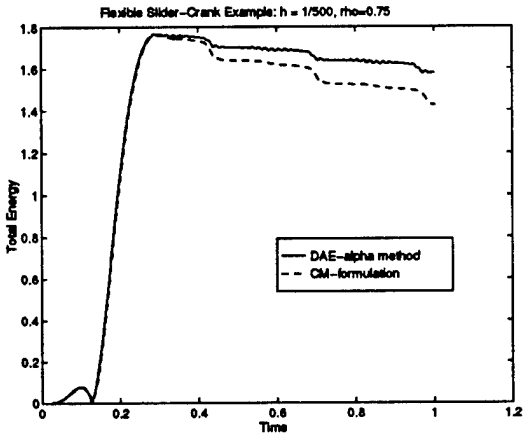

Figure 4.11: Total Energy Comparison, CM vs. Stabilized Index-2 DAE

References

[1] K. E. Brenan, S. L. Campbell, and L. R. Petzold, *Numerical Solution of Initial-Value Problems in Differential-Algebraic Equations*, second edition, SIAM, 1995.

[2] A. Cardona and M. Géradin, *Time integration of the equations of motion in mechanical analysis*, Computers & Struct., 33 (1989), pp. 801-820.

[3] J. Chung and G. M. Hulbert, *A time integration algorithm for structural dynamics with improved numerical dissipation: The generalized-α method*, ASME J. Appl. Mech., No. 93-APM-20, 1993.

[4] R. R. Craig, Jr.,*Structural Dynamics - An Introduction to Computer Methods*, Wiley, 1981.

[5] C. Führer and B.J. Leimkuhler, *Numerical solution of differential-algebraic equations for constrained mechanical motion*, Numer. Math. 59 (1991), pp. 55-69.

[6] C.W. Gear, G.K. Gupta and B.J. Leimkuhler, *Automatic integration of the Euler-Lagrange equations with constraints*, J. Comp. Appl. Math., 12 (1985), pp. 77-90.

[7] G. H. Golub and C. F. Van Loan, *Matrix Computations, second edition*, Johns Hopkins University Press, 1989.

[8] E. Griepentrog and R. März, *Differential-Algebraic Equations and their Numerical Treatment*, Teubner, Leipzig, 1986.

[9] E. Hairer and G. Wanner, *Solving Ordinary Differential Equations II: Stiff and Differential- Algebraic Problems*, Springer-Verlag, Berlin, 1991.

[10] E. J. Haug, *Computer Aided Kinematics and Dynamics of Mechanical Systems Volume I: Basic Methods*, Allyn-Bacon, 1989.

[11] H. H. Hilber, T. J. R. Hughes and R. L. Taylor, *Improved numerical dissipation for time integration algorithms in structural dynamics*, Earthquake Engineering and Structural Dynamics 5 (1977), pp. 283-292.

[12] C. Hoff and P.J. Pahl, *Development of an implicit method with numerical dissipation from a generalized single-step algorithm for structural dynamics*, Comp. Meth. in Appl. Mech. and Eng., 67 (1988), pp. 367-385.

[13] L. Jay, *Convergence of a class of Runge-Kutta methods for differential-algebraic systems of index 2*, BIT 33 (1993), pp. 137-150.

[14] T.R. Kane and D. A. Levinson, *Dynamics: Theory and Applications*, McGraw-Hill, New York, 1985.

[15] Ch. Lubich, *Extrapolation integrators for constrained multibody systems*, IMPACT of Comp. Sci. Engr., 3 (1991), pp. 213-234.

[16] Ch. Lubich, *Integration of stiff mechanical systems by Runge-Kutta methods*, ZAMP, 44 (1993), pp. 1022-1053.

[17] N. M. Newmark, *A method of computation for structural dynamics*, ASCE J. Eng. Mech. Div., 85 (1959), pp. 67-94.

[18] F. Potra and W.C. Rheinboldt, *On the numerical solution of the Euler-Lagrange equations*, J. Mech. Struct. Mach., 19 (1991), pp. 1-18.

[19] M.S. Pereira and J. A.C. Ambrósio, Editors, *Computer Aided Analysis of Rigid and Flexible Mechanical Systems*, NATO-Advanced Study Institute, Tróia, Portugal, 27 June- 9 July, 1993.

[20] R.E. Roberson and R. Schwertassek, *Dynamics of Multibody Systems*. Springer, Berlin, 1988.

[21] W. Schiehlen, Editor, *Advanced Multibody System Dynamics*, Kluwer Academic Publishers, Stuttgart, 1993.

[22] B. Simeon, *Modelling of a flexible slider crank mechanism by a mixed system of DAEs and PDEs*, Tech. Rept., Fachbereich Mathematik, Technische Hochschule Darmstadt, Darmstadt, Germany, 1995.

[23] R.A. Wehage and E. J. Haug, *Generalized coordinate partitioning for dimension reduction in analysis of constrained dynamic systems*, ASME J. Mech. Design, 134 (1982), pp. 247-255.

[24] J. Yen, *Constrained equations of motion in multibody dynamics as ODEs on manifolds*, SINUM, 30 (1993), pp. 553-568.

[25] J. Yen and L.R. Petzold, *Numerical Solution of nonlinear oscillatory multibody dynamic systems*, Proceedings of the 1995 Biennial Conference on Numerical Analysis, Editors D. F. Griffiths and G. A. Watson, Pitman Research Notes in Mathematics, Vol. 344 (1996), Addison Wesley Longman Ltd, pp. 209-225.

[26] J. Yen and L.R. Petzold, *A efficient Newton-type iteration for the numerical solution of highly oscillatory constrained multibody dynamic systems*, Tech. Rept. TR-96-001, AHPCRC, Univ. of Minnesota, submitted to SISC, 1996.

[27] W.S. Yoo and E.J. Haug, *Dynamics of articulated structures, part I theory*, J. Struct. Mech., 14(1), 1986, pp. 105-126.

[28] W.L. Wood, M. Bossak, and O.C. Ziekiewicz, *An alpha modification of Newmark's method*, Int. J. Numer. Meth. in Engr., 15 (1980), pp. 1562-1566.